

3D-GPT: PROCEDURAL 3D MODELING WITH LARGE LANGUAGE MODELS

Chunyi Sun^{1*}, Junlin Han^{2,3*}, Weijian Deng¹, Xinlong Wang⁴, Zishan Qin¹, Stephen Gould¹

¹Australian National University, ²University of Oxford, ³Cybever, ⁴Beijing Academy of Artificial Intelligence

Project page: <https://chunyi1.github.io/3DGPT/3dgpt.html>

* Equal contribution

ABSTRACT

In the pursuit of efficient automated content creation, procedural generation, leveraging modifiable parameters and rule-based systems, emerges as a promising approach. Nonetheless, it could be a demanding endeavor, given its intricate nature necessitating a deep understanding of rules, algorithms, and parameters. To reduce workload, we introduce 3D-GPT, a framework utilizing large language models (LLMs) for instruction-driven 3D modeling. 3D-GPT positions LLMs as proficient problem solvers, dissecting the procedural 3D modeling tasks into accessible segments and appointing the apt agent for each task. 3D-GPT integrates three core agents: the task dispatch agent, the conceptualization agent, and the modeling agent. They collaboratively achieve two objectives. First, it enhances concise initial scene descriptions, evolving them into detailed forms while dynamically adapting the text based on subsequent instructions. Second, it integrates procedural generation, extracting parameter values from enriched text to effortlessly interface with 3D software for asset creation. Our empirical investigations confirm that 3D-GPT not only interprets and executes instructions, delivering reliable results but also collaborates effectively with human designers. Furthermore, it seamlessly integrates with Blender, unlocking expanded manipulation possibilities. Our work highlights the potential of LLMs in 3D modeling, offering a basic framework for future advancements in scene generation and animation.

1 INTRODUCTION

In the metaverse era, 3D content creation serves as a catalyst for transformative progress, redefining multimedia experiences in domains like gaming, virtual reality, and cinema with intricately crafted models. Yet, designers often grapple with a time-intensive 3D modeling process, starting from basic shapes (*e.g.*, cubes, spheres, or cylinders) and employing software like Blender for meticulous shaping, detailing, and texturing. This demanding workflow concludes with rendering and post-processing to deliver the polished final model. While procedural generation holds promise with its efficiency in automating content creation through adjustable parameters and rule-based systems (Deitke et al., 2022; Greff et al., 2022; He et al., 2021; Jiang et al., 2018; Raistrick et al., 2023), it demands a comprehensive grasp of generation rules, algorithmic frameworks, and individual parameters. Furthermore, aligning these processes with the creative visions of clients, through effective communication, adds another layer of complexity. This underscores the importance of simplifying the traditional 3D modeling workflow to empower creators in the metaverse era.

LLMs have showcased exceptional language understanding capabilities, including planning and tool utilization (Imani et al., 2023; Zhang et al., 2023a; Gong et al., 2023; Zeng et al., 2022).

Furthermore, LLMs demonstrate outstanding proficiency in characterizing object attributes, such as structure and texture (Menon & Vondrick, 2022; Pratt et al., 2022; Fan et al., 2023), enabling them to enhance details from rough descriptions. Additionally, they excel at parsing concise textual information and comprehending intricate code functions, while seamlessly facilitating efficient interactions with users. Driven by these extraordinary capabilities, we embark on exploring their innovative applications in procedural 3D modeling. Our primary objective is to harness the power of LLMs to exert control over 3D creation software in accordance with the requirements of clients.

In pursuit of this vision, we introduce 3D-GPT, a framework aimed at facilitating instruction-driven 3D content synthesis. 3D-GPT enables LLMs to function as problem-solving agents, breaking down the 3D modeling task into smaller, manageable components, and determining when, where, and how to accomplish each segment. 3DGPT comprises three key agents: conceptualization agent, 3D modeling agent and task dispatch agent. The first two agents collaborate harmoniously to fulfill the roles of 3D conceptualization and 3D modeling by manipulating the 3D generation functions. Subsequently, the third agent manages the system by taking the initial text input, handling subsequence instructions, and facilitating effective cooperation between the two aforementioned agents.

By doing so, they work toward two key objectives. First, it enhances initial scene descriptions, guiding them towards more detailed and contextually relevant forms while adapting the textual input based on subsequent instructions. Second, instead of directly crafting every element of 3D content, we employ procedural generation, making use of adaptable parameters and rule-based systems to interface with 3D software. Our 3D-GPT is equipped with the capability to understand procedural generation functions and extract corresponding parameter values from the enriched text.

3D-GPT offers controllable and precise 3D generation guided by users’ textual descriptions. It reduces the workload of manually defining each controllable parameter in procedural generation, particularly within complex scenes that encompass diverse aspects. Moreover, 3D-GPT enhances collaboration with users, making the creative process more efficient and user-centric. Furthermore, 3D-GPT seamlessly interfaces with Blender, granting users diverse manipulation capabilities: object transformations, material adjustments, primitive additions, object animations, mesh editing, and physical motion simulations. Based on our experiments, we posit that LLMs exhibit the potential to handle more intricate visual inputs. Our contributions are summarized as follows:

- Introducing 3D-GPT, a training-for-free framework designed for 3D scene generation. Our approach leverages the innate multimodal reasoning capabilities of LLMs, streamlining the efficiency of end-users engaged in procedural 3D modeling.
- Exploration of an alternative path in text-to-3D generation, wherein our 3D-GPT generates Python codes to control 3D software, potentially offering increased flexibility for real-world applications.
- Empirical experiments demonstrate the substantial potential of LLMs in terms of their reasoning, planning, and tool-using capabilities in 3D content generation.

2 RELATED WORK

2.1 TEXT-TO-3D GENERATION

With the recent advance in text-to-image generation modeling, there has been a growing interest in text-to-3D generation (Sanghi et al., 2022; Poole et al., 2022; Lin et al., 2023; Xu et al., 2023; Metzger et al., 2023; Wang et al., 2023; Xu et al., 2023; Mohammad Khalid et al., 2022; Jain et al., 2022). The common paradigm of them is to perform per-shape optimization with differentiable rendering and the guidance of the CLIP model (Radford et al., 2021) or 2D diffusion models (Rombach et al., 2022). For example, DreamFields (Jain et al., 2022) and CLIP-Mesh (Mohammad Khalid et al., 2022) explore zero-shot 3D content creation using only CLIP guidance. Dreamfusion (Poole et al., 2022) optimizes NeRF Mildenhall et al. (2021) with the guidance of a text-to-image diffusion model, achieving remarkable text-to-3D synthesis results. To address optimization speed and visual quality challenges, Magic3D (Lin et al., 2023) uses low-resolution diffusion priors and a sparse 3D hash grid for speed, alongside an efficient differentiable render for textured 3D mesh model optimization. To enhance the fidelity of generated 3D models, innovative approaches refine the 3D geometry. For instance, Dream3D (Xu et al., 2023) directly initializes NeRF using a generated Signed Distance Function (SDF) for better geometry control. Latent-NeRF (Metzger et al., 2023) incorporates a user-provided mesh for direct occupancy loss during geometry optimization in NeRF. Subject-driven text-to-3D generation is gaining traction for personalized synthesis (Raj et al., 2023; Liu et al., 2023; Melas-Kyriazi et al., 2023). It creates subject-specific 3D assets based on input images and text prompts. To achieve this, DreamBooth3D (Raj et al., 2023) proposes a 3-stage optimization strategy to jointly leverage the 3D consistency of NeRF together with the personalizing capability of the text-to-image diffusion model. One-2-3-45 (Liu et al., 2023) uses a view-conditioned 2D diffusion model (Zero123) to generate multi-view images for learning SDF-based generalizable neural surface reconstruction. Unlike the above approaches, our objective is not to generate conventional

neural representations as the final 3D output. Instead, we utilize LLMs to generate Python code that controls Blender’s 3D modeling based on the provided instructions.

2.2 LARGE LANGUAGE MODELS

Large language models (LLMs) are a promising approach to capture and represent the compressed knowledge and experiences of humans, projecting them into language space (Devlin et al., 2018; Raffel et al., 2020; OpenAI, 2023; Chowdhery et al., 2022; Bubeck et al., 2023). LLMs have consistently showcased remarkable performance extending beyond canonical language processing domains. They exhibit the capability to address intricate tasks that were once considered the exclusive domain of specialized algorithms or human experts. These tasks encompass areas such as mathematical reasoning (Imani et al., 2023; Wei et al., 2022), medicine (Jeblick et al., 2022; Yang et al., 2023), and planning (Zhang et al., 2023a; Gong et al., 2023; Huang et al., 2023; 2022) For instance, Huang et al. (2022) leverage the LLMs’ internet-scale domain knowledge and emergent zero-shot planning abilities to perform complex task planning and reasoning. Gong et al. (2023) explore LLMs in multi-agent coordination in scenarios encompassing multiple task objectives. (Zeng et al., 2022) introduce a modular framework that leverages structured dialogue via prompting between multiple large pre-trained models to make joint predictions for new multimodal tasks, without requiring finetuning. Moreover, specialized LLMs for particular applications have been explored such as Codex (Chen et al., 2021) for Python code generation, Galactica (Taylor et al., 2022) for scientific knowledge, and LaMDA (Thoppilan et al., 2022) for dialogue applications. This work explores the innovative application of LLMs in 3D modeling, employing them to control 3D procedural generation.

3 3D-GPT

3.1 TASK FORMULATION

The overall objective is the generation of 3D content based on a sequence of natural language instructions, denoted as $\mathcal{L} = [L_i]$. The initial instruction, designated as L_0 , serves as a comprehensive description of the 3D scene, such as “*A misty spring morning, where dew-kissed flowers dot a lush meadow surrounded by budding trees*”. Subsequent instructions are employed to modify the existing scene, as exemplified by instructions like “*Transform the white flowers into yellow flower*” or “*translate the scene into a winter setting*”.

To accomplish this objective, we introduce a framework named 3D-GPT, which empowers LLMs to act as problem-solving agents. We point out that employing LLMs to directly create every element of 3D content poses significant challenges. LLMs lack specific pre-training data for proficient 3D modeling and, as a result, may struggle to accurately determine which elements to modify and how to modify them based on given instructions.

To avoid this challenge, we employ procedural generation to control the 3D content creation. It makes use of adaptable parameters and rule-based systems to interface with 3D software (*e.g.*, Blender) so as to efficiently conduct 3D modeling (Deitke et al., 2022; Greff et al., 2022; He et al., 2021; Jiang et al., 2018; Raistrick et al., 2023).

Our approach conceptualizes the 3D procedural generation engine as a set of functions, denoted as $\mathcal{F} = \{F_j\}$, where each function F_j takes parameters P_j as input.

Within the 3D-GPT framework, for each instruction L_i , we frame the modeling task as the selection of a subset $\hat{\mathcal{F}} \subseteq \mathcal{F}$, combined with the inference of corresponding parameters P_j for each function F_j in this subset. The ultimate aim is to ensure that the $\hat{\mathcal{F}}$ collaboratively generates a 3D scene that aligns with the descriptions provided in \mathcal{L} . By adeptly addressing both function selection and parameter inference for every sub-instruction L_i , 3D-GPT generates a Python script file with the capacity to manipulate Blender’s 3D modeling environment, thereby proficiently meeting the user’s specified requirements outlined in the instruction sequence \mathcal{L} .

3.2 MODELING TOOL PREPARATION

In our framework, we utilize Infinigen Raistrick et al. (2023), a Python-Blender-based procedural generator equipped with a rich library of generation functions. To empower LLMs with the ability

to proficiently leverage Infinigen, we provide crucial prompts for each function F_j . These prompts encompass function documentation D_j , easily understandable code C_j , required information I_j , and a usage example E_j :

- D_j : it entails a comprehensive explanation of the input parameter P_j , coupled with a clear elucidation of the function’s purpose and functionality.
- C_j : we present meticulously restructured and highly readable function code, ensuring that it is accessible and comprehensible for LLMs.
- I_j : this component outlines the specific information required to infer the function parameters, thereby assisting LLMs in understanding the context and prerequisites of each function. For example, in the case of a flower generation function, I_j indicates the required visual properties for modeling, such as flower color, flower petal appearance (e.g., size, curve, and length), and flower center appearance.
- E_j : we provide illustrative examples to demonstrate how to infer the parameter P_j from the accompanying text descriptions and subsequently invoke the function. Continuing with the example of a flower generation function, E_j includes a practical demonstration of how to infer the parameters and call the function based on input text like “a sunflower.”

By providing LLMs with these resources, we enable them to leverage their core competencies in planning, reasoning, and tool utilization. As a result, LLMs can effectively harness Infinigen for 3D generation based on language instructions in a seamless and efficient manner.

3.3 MULTI-AGENTS FOR 3D REASONING, PLANING AND TOOL USING

Upon tool preparation, 3D-GPT employs a multi-agent system to tackle the procedural 3D modeling task. This system comprises three integral agents: the task dispatch agent, the conceptualization agent, and the modeling agent, illustrated in Figure 1. Together, they deconstruct the procedural 3D modeling task into manageable segments, with each agent specializing in distinct aspects: 3D reasoning, planning, and tool utilization. The task dispatch agent plays a pivotal role in the planning process. It leverages user instructions to query function documents and subsequently selects the requisite functions for execution. Once functions are selected, the conceptualization agent engages in reasoning to enrich the user-provided text description. Building upon this, the modeling agent deduces the parameters for each selected function and generates Python code scripts to invoke Blender’s API, facilitating the creation of the corresponding 3D content. Additionally, images can be rendered using Blender rendering capability.

Task Dispatch Agent for Planing. The Task Dispatch Agent, armed with comprehensive information of all available functions \mathcal{F} within the procedural generation, efficiently identifies the requisite functions for each instructional input. For instance, when presented with an instruction such as “translate the scene into a winter setting”, it pinpoints functions like `add_snow_layer()` and `update_trees()`. This pivotal role played by the task dispatch agent is instrumental in facilitating efficient task coordination between the conceptualization and modeling agents. Without it, the conceptualization and the modeling agents have to analyze all provided functions \mathcal{F} for each given instruction. This not only increases the workload for these agents but also extends processing time and can potentially lead to undesired modifications.

The communication flow between the LLM system, the user, and the task dispatch agent is outlined as follows:

<p>— LLM System: You are a proficient planner for selecting suitable functions based on user instructions. You are provided with the following functions: $\langle (F_j^{name}, F_j^{usage}) \rangle$. Below are a few examples of how to choose functions based on user instructions: $\langle E_j^{\text{task.dispatch}} \rangle$.</p> <p>— User: My instruction is: $\langle L_i \rangle$.</p> <p>— Task Dispatch Agent: Given the instruction $\langle L_i \rangle$, we determine the sublist of functions $\hat{\mathcal{F}}$ that need to be used for 3D modeling.</p>
--

In this context, $\langle (F_j^{name}, F_j^{usage}) \rangle$ represents a list of function names and concise function usage descriptions for all available functions and examples $\langle E_{\text{task.dispatch}} \rangle$ provide guided examples for prompt-based instructions.

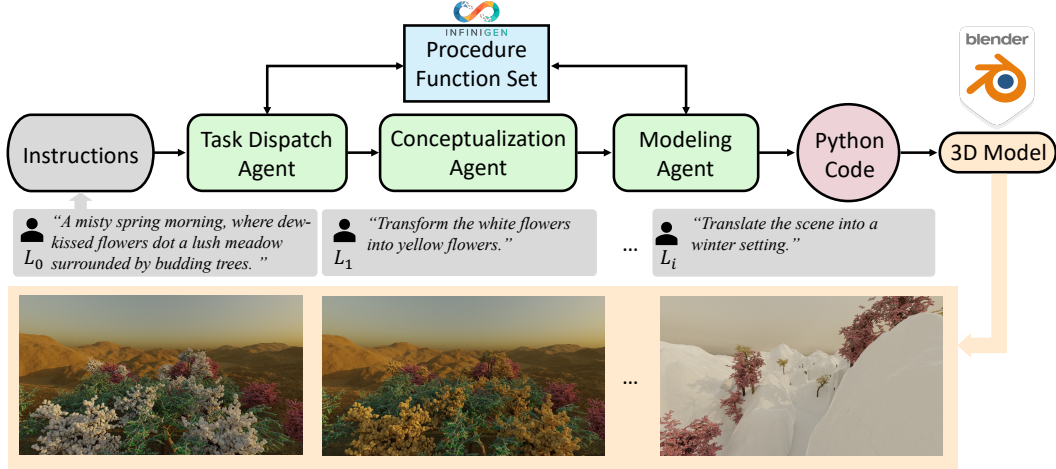


Figure 1: **3D-GPT Overview.** 3D-GPT employs LLMs as a multi-agent system with three collaborative agents for procedural 3D generation. These agents consult documents from the procedural generator, infer function parameters, and produce Python code. The generated code script interfaces with Blender’s API for 3D content creation and rendering.

Engaging the Conceptualization Agent for Reasoning. The description may not explicitly provide the detailed appearance descriptions needed for modeling. For instance, consider the description: “*A misty spring morning, where dew-kissed flowers dot a lush meadow surrounded by budding trees*”. When employing a tree modeling function that necessitates parameters such as tree branch length, tree size, and leaf type, it becomes apparent that these specific details are not directly stated in the given text. When instructing the modeling agent to infer parameters directly, it tends to provide simplistic solutions, like using default or reasonable values from the parameter document or copying values from prompting examples. This reduces diversity in generation and complicates parameter inference.

To alleviate this issue, we introduce the conceptualization agent which collaborates with the task dispatch agent to augment the user-provided text description (L_i). After the task dispatch agent selects the required functions, we send the user input text and the corresponding function-specific information to the conceptualization agent and request augmented text. For each function F_j , it enriches L_i into detailed appearance descriptions L_i^j . The communication between the system and the Conceptualization Agent for instruction $< L_i >$ and function $< F_j >$ is as follows:

— **LLM System:** You are a skilled writer, especially when it comes to describing the appearance of objects and large scenes. Given a description $< L_i >$, provide detailed descriptions for the following information $< I_j >$. For terms not mentioned in the description, use your imagination to ensure they fit the text description.
— **Conceptualization Agent:** Given the $< L_i >$ and requested information $< I_j >$, the extended description is: $< \widehat{L}_i^j >$.

Modeling Agent for Tool Using. After conceptualization, the 3D modeling processing is targeted to convert the detailed human language to machine-understandable language.

In our framework, our modeling agent manipulates the functions of procedural modeling in the library to create a realistic 3D model. For each function F_j and user instruction L_i , the task dispatch agent receive augmented context \widehat{L}_i^j from the conceptualization agent. For each function F_j , we have the code C_j , function documentation D_j , and one usage example E_j . The modeling agent utilizes this information to select the appropriate functions and deduce the corresponding parameters. Subsequently, the modeling agent generates Python code that accurately calls the selected function (e.g., call it in the loop, not call) and correctly passes the inferred parameters with the appropriate data types to the function.

The two-turn utterances are based on the following pattern:

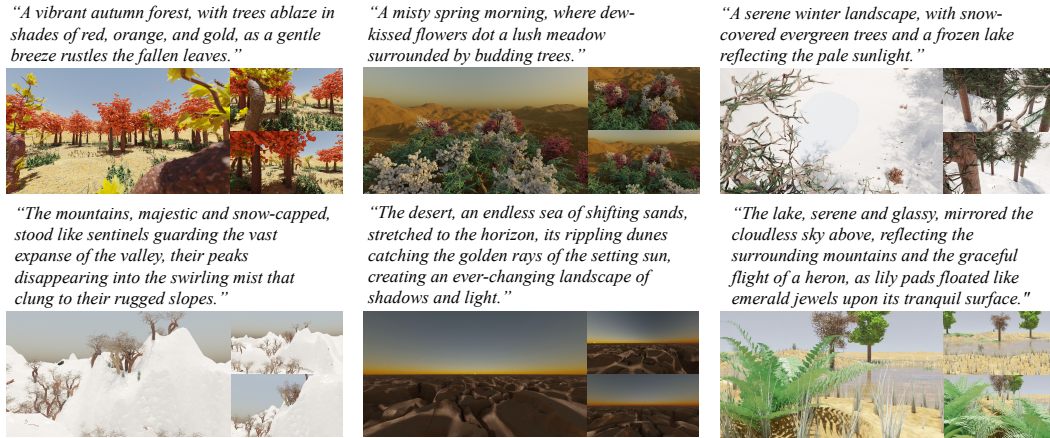


Figure 2: Visual Examples of Instruction-Based 3D Scene Generation. 3D-GPT can construct large 3D scenes that align with the provided initial instruction. We demonstrate that the rendered images contain various visual factors in line with the given instructions.

— **LLM System:** You are a good 3D designer who can convert long text descriptions into parameters, and is good at understanding Python functions to manipulate 3D content. Given the text description $\langle L_i^f \rangle$, we have the following function codes $\langle C_j \rangle$ and the document for function $\langle D_j \rangle$. Below is an example bout how to make function calls to model the scene to fit the description: $\langle E_{j, \text{modeling}} \rangle$. Understand the function, and model the 3D scene that fits the text description by making a function call.
— **Modeling Agent:** Given the description $\langle L_i^j \rangle$, we use the following functions: ..., and their respective parameter values ... are adopted.

Blender Rendering. The Modeling agent ultimately supplies the Python function calls with inferred parameters, which are employed for Blender node control and rendering, resulting in the production of the final 3D mesh and RGB results.

4 EXPERIMENTS

Our experimentation begins by showcasing the proficiency of 3D-GPT in consistently generating results that align with user instructions, encompassing scenarios involving both large scenes and individual objects. Subsequently, we delve into specific examples to illustrate how our agents effectively comprehend tool functionalities, access necessary knowledge, and employ it for precise control. To deepen our understanding, we conduct an ablation study to systematically examine the contributions of each agent within our multi-agent system.

4.1 3D MODELING

Large Scene Generation. We investigate the capability of 3DGPT to control modeling tools based on scene descriptions *without any training*. To conduct this experiment, we generated 100 scene descriptions using ChatGPT with the following prompt: “*You are a good writer, provide 10 different natural scene descriptions for me*”. We collected responses to this prompt 10 times to form our dataset. In Figure 2, we present the multi-view rendering results of 3D-GPT. These results indicate that our approach is capable of generating large 3D scenes that generally align well with the provided text descriptions, showcasing a noticeable degree of diversity. Notably, all 3D outcomes are directly rendered using Blender, ensuring that all meshes are authentic, thereby enabling our method to achieve absolute 3D consistency and produce real ray-tracing rendering results.

Fine-detail Control for Single Class. Apart from generating large scenes from concise descriptions, we assess the capabilities of 3D-GPT for modeling objects. We evaluate crucial factors such as curve modeling, shape control, and an in-depth understanding of object appearances. To this end,



Figure 3: Single Class Control Result. Our method effectively acquires the necessary knowledge for modeling, enabling precise object control in terms of shape, curve, and key appearance capture. The generated results closely align with the given text.

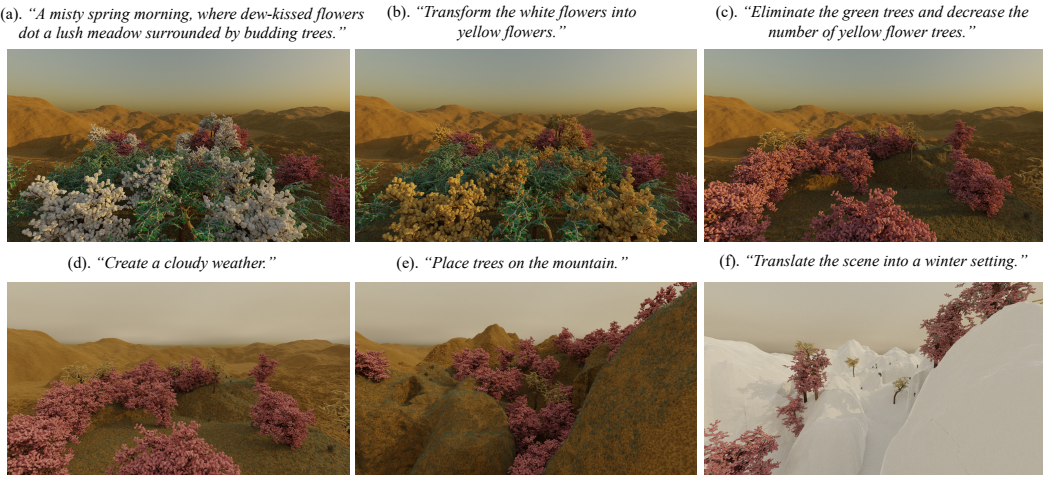


Figure 4: Subsequence Instruction Editing Result. (a) Initial instruction-generated scene. (b)-(f) Sequential editing steps with corresponding instructions. Our method enables controllable editing and effective user-agent communication.

we report the results of fine-grained object control. This includes nuanced aspects such as object curves, key appearance features, and color, all derived from input text descriptions. We employ random prompts to instruct GPT for various real-world flower types. As depicted in Figure 3, our method adeptly models each flower type, faithfully capturing their distinct appearances. This study underscores the potential of 3D-GPT in achieving precise object modeling and fine-grained attribute control of object types and visual characteristics.

Subsequence Instruction Editing. Here, we test the ability of 3D-GPT for effective human-agent communication and task manipulation. In Figure 4, we observe that our method can comprehend subsequence instructions and make accurate decisions for scene modification. Note that, unlike the existing text-to-3D methods, 3D-GPT maintains a memory of all prior modifications, thereby facilitating the connection of new instructions with the scene’s context. Furthermore, our method eliminates the need for additional networks for controllable editings Zhang et al. (2023b). This study underscores the efficiency and versatility of 3D-GPT in adeptly handling complex subsequence instructions for 3D modeling.

Individual Function Control. To evaluate the effectiveness of 3D-GPT in tool utilization, we present an illustrative example that highlights our method’s ability to control individual functions and infer parameters. Figure 5 exemplifies the capability of 3D-GPT to model sky appearances based on input text descriptions. It is worth noting that the function responsible for generating the sky texture does not directly correlate color information with sky appearance. Instead, it relies on



Figure 5: **Single Function Control Result.** Visual result (top) and modeling agent response example (bottom). Our method demonstrates a high degree of accuracy in inferring algorithm parameters, even when they do not possess a direct connection to visual appearance.

the Nishita-sky modeling method, which requires a profound understanding of real-world sky and weather conditions, considering input parameters. Our method adeptly extracts crucial information from the textual input and comprehends how each parameter influences the resulting sky appearance, as evident in Figure 5 (c) and (d). These results demonstrate that our method can effectively use individual functions as well as infer corresponding parameters.

4.2 ABLATION STUDY

We conduct separate ablation studies for the Conceptualization Agent and Task Dispatch Agent. Our assessment focused on CLIP scores (Radford et al., 2021), failure rates, and parameter diversity, quantified using the categorical Shannon Diversity Index. The CLIP score measures the alignment between text and generated images. The failure rate represents the percentage of system failures due to issues such as incorrect datatypes, wrong response patterns, or missing parameters from the Modeling Agent. Parameter diversity aims to gauge the diversity of generated outputs.

Metrics/ Method	CLIP Score
w/o TDA	22.79
Ours	29.16

(a) **Ablation Study of Task Dispatch Agent.**

Metrics/ Method	CLIP Score	Failure Rate	Parameter Diversity
w/o CA	21.51	3.6%	6.32
Ours	30.30	0.8%	7.34

(b) **Ablation Study of Conceptualization Agent.**

Table 1: **Ablation Study.** "w/o CA" indicates without the Conceptualization Agent, "w/o TDA" indicates without the Task Dispatch Agent.

Case Study of Task Dispatch Agent. For the Task Dispatch Agent, the CLIP score is measured using 100 initial scene descriptions, each appended with one additional subsequence instruction for each scene. Table 1 (a) shows that without the Task Dispatch Agent, the CLIP score dropped from 29.16 to 22.79. It is important to note that the Task Dispatch Agent primarily impacts the performance of subsequence instructions, as all functions are utilized for the initial instruction. These findings underscore the pivotal role of the Task Dispatch Agent in managing communication flow.

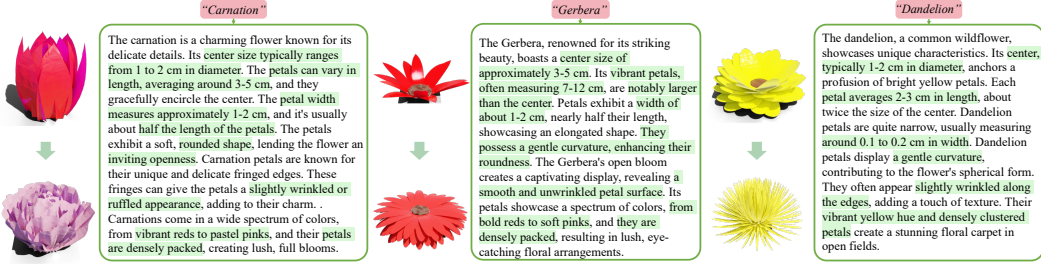


Figure 6: **Conceptualization Agent Case Study.** The enriched textual evidence demonstrates that the Conceptualization Agent provides essential knowledge for parameter inference (highlighted in green). For each subfigure, we compare the 3D model without (Top) and with (Bottom) agent. The models generated with the agent better match the text description than those without it.

Case Study of conceptualization Agent. For the Conceptualization Agent, the CLIP score is measured using 100 initial scene descriptions. Table 1 (b) displays the results, indicating that without the Conceptualization Agent, both text alignments (CLIP score) and parameter diversity decreased significantly. Moreover, the failure rate increased substantially, which adversely impacts the efficiency of the entire modeling process. Figure 6 illustrates how the Conceptualization Agent facilitates the acquisition of essential knowledge for 3D modeling, providing a visual comparison of results with and without its involvement. When the Conceptualization Agent is engaged, the generated results closely align with the appearance of the intended flower type, highlighting its invaluable contribution to elevating overall 3D generation quality and fidelity.

5 DISCUSSION AND CONCLUSION

We have introduced 3D-GPT, a novel training-free framework for instruction-driven 3D modeling seamlessly integrated with procedural generation. Leveraging the capabilities of LLMs, 3DGPT aims to enhance human-AI communication in the context of 3D design. Our approach involves the collaborative efforts of three agents functioning as a cohesive 3D modeling team, ultimately yielding a 3D modeling file as output, as opposed to conventional 3D neural representations. Moreover, our method consistently delivers high-quality results, showcases adaptability to expansive scenes, ensures 3D consistency, provides material modeling and editing capabilities, and facilitates real ray tracing for achieving lifelike visualizations. Our empirical experiments show the potential of LLMs for reasoning, planning, and tool using in procedural 3D modeling.

Limitations and Potential Directions. While our framework has demonstrated promising 3D modeling results closely aligned with user instructions, it is essential to acknowledge several limitations: 1) Limited curve control and shading design: Currently, our framework lacks advanced capabilities for precise curve control and intricate shading design. Tasks involving the manipulation of tree branches or the blending of colors for leaf textures remain challenging. 2) Dependence on procedural generation algorithms: the effectiveness of our framework is contingent on the quality and availability of procedural generation algorithms. This reliance may limit results in specific categories, such as hair and fur. 3) Handling multi-modal instructions: challenges arise in processing multi-modal instructions, including audio and image inputs, potentially leading to information loss. These limitations offer valuable insights for shaping future research and development in the field. We highlight three compelling directions for future investigation:

LLM 3D Fine-Tuning: It is promising to fine-tune LLMs to enhance their capabilities in geometry control, shading design, and fine-texture modeling. This refinement will make LLMs more adept at handling intricate 3D modeling tasks and grant greater creative control over the resulting 3D scenes.

Autonomous Rule Discovery: Building on the demonstrated tool-making capabilities of LLMs, one direction is to develop an autonomous 3D modeling system that reduces human involvement. This could empower LLMs to autonomously discover generation rules for new object classes and scenes, thus expanding the creative potential.

Multi-Modal Instruction Processing: To achieve more comprehensive and expressive 3D modeling based on varied user inputs, it is crucial to enhance the system's ability to comprehend and respond to multi-modal instructions. This would facilitate richer and more diverse 3D modeling outcomes, shaped by a broader spectrum of user inputs.

REFERENCES

- Sébastien Bubeck, Varun Chandrasekaran, Ronen Eldan, Johannes Gehrke, Eric Horvitz, Ece Kamar, Peter Lee, Yin Tat Lee, Yuanzhi Li, Scott Lundberg, Harsha Nori, Hamid Palangi, Marco Tulio Ribeiro, and Yi Zhang. Sparks of artificial general intelligence: Early experiments with GPT-4. *arXiv preprint arXiv:2303.12712*, 2023.
- Mark Chen, Jerry Tworek, Heewoo Jun, Qiming Yuan, Henrique Ponde de Oliveira Pinto, Jared Kaplan, Harri Edwards, Yuri Burda, Nicholas Joseph, Greg Brockman, Alex Ray, Raul Puri, Gretchen Krueger, Michael Petrov, Heidy Khlaaf, Girish Sastry, Pamela Mishkin, Brooke Chan, Scott Gray, Nick Ryder, Mikhail Pavlov, Alethea Power, Lukasz Kaiser, Mohammad Bavarian, Clemens Winter, Philippe Tillet, Felipe Petroski Such, Dave Cummings, Matthias Plappert, Fotios Chantzis, Elizabeth Barnes, Ariel Herbert-Voss, William Hebgen Guss, Alex Nichol, Alex Paino, Nikolas Tezak, Jie Tang, Igor Babuschkin, Suchir Balaji, Shantanu Jain, William Saunders, Christopher Hesse, Andrew N. Carr, Jan Leike, Josh Achiam, Vedant Misra, Evan Morikawa, Alec Radford, Matthew Knight, Miles Brundage, Mira Murati, Katie Mayer, Peter Welinder, Bob McGrew, Dario Amodei, Sam McCandlish, Ilya Sutskever, and Wojciech Zaremba. Evaluating large language models trained on code. *arXiv preprint arXiv:2107.03374*, 2021.
- Aakanksha Chowdhery, Sharan Narang, Jacob Devlin, Maarten Bosma, Gaurav Mishra, Adam Roberts, Paul Barham, Hyung Won Chung, Charles Sutton, Sebastian Gehrmann, Parker Schuh, Kensen Shi, Sasha Tsvyashchenko, Joshua Maynez, Abhishek Rao, Parker Barnes, Yi Tay, Noam Shazeer, Vinodkumar Prabhakaran, Emily Reif, Nan Du, Ben Hutchinson, Reiner Pope, James Bradbury, Jacob Austin, Michael Isard, Guy Gur-Ari, Pengcheng Yin, Toju Duke, Anselm Levskaya, Sanjay Ghemawat, Sunipa Dev, Henryk Michalewski, Xavier Garcia, Vedant Misra, Kevin Robinson, Liam Fedus, Denny Zhou, Daphne Ippolito, David Luan, Hyeontaek Lim, Barret Zoph, Alexander Spiridonov, Ryan Sepassi, David Dohan, Shivani Agrawal, Mark Omernick, Andrew M. Dai, Thanumalayan Sankaranarayana Pillai, Marie Pellat, Aitor Lewkowycz, Erica Moreira, Rewon Child, Oleksandr Polozov, Katherine Lee, Zongwei Zhou, Xuezhi Wang, Brennan Saeta, Mark Diaz, Orhan Firat, Michele Catasta, Jason Wei, Kathy Meier-Hellstern, Douglas Eck, Jeff Dean, Slav Petrov, and Noah Fiedel. PaLM: Scaling language modeling with pathways. *arXiv preprint arXiv:2204.02311*, 2022.
- Matt Deitke, Eli VanderBilt, Alvaro Herrasti, Luca Weihs, Kiana Ehsani, Jordi Salvador, Winson Han, Eric Kolve, Aniruddha Kembhavi, and Roozbeh Mottaghi. ProcTHOR: Large-scale embodied ai using procedural generation. *Advances in Neural Information Processing Systems*, 35: 5982–5994, 2022.
- Jacob Devlin, Ming-Wei Chang, Kenton Lee, and Kristina Toutanova. BERT: Pre-training of deep bidirectional transformers for language understanding. *arXiv preprint arXiv:1810.04805*, 2018.
- Lijie Fan, Dilip Krishnan, Phillip Isola, Dina Katabi, and Yonglong Tian. Improving clip training with language rewrites. *arXiv preprint arXiv:2305.20088*, 2023.
- Ran Gong, Qiuyuan Huang, Xiaojian Ma, Hoi Vo, Zane Durante, Yusuke Noda, Zilong Zheng, Song-Chun Zhu, Demetri Terzopoulos, Li Fei-Fei, and Jianfeng Gao. MindAgent: Emergent gaming interaction. *arXiv preprint arXiv:2309.09971*, 2023.
- Klaus Greff, Francois Belletti, Lucas Beyer, Carl Doersch, Yilun Du, Daniel Duckworth, David J Fleet, Dan Gnanapragasam, Florian Golemo, Charles Herrmann, Thomas Kipf, Abhijit Kundu, Dmitry Lagun, Issam Laradji, Hsueh-Ti (Derek) Liu, Henning Meyer, Yishu Miao, Derek Nowrouzezahrai, Cengiz Oztireli, Etienne Pot, Noha Radwan, Daniel Rebain, Sara Sabour, Mehdi S. M. Sajjadi, Matan Sela, Vincent Sitzmann, Austin Stone, Deqing Sun, Suhani Vora, Ziyu Wang, Tianhao Wu, Kwang Moo Yi, Fangcheng Zhong, and Andrea Tagliasacchi. Kubric: A scalable dataset generator. In *Proceedings of the IEEE/CVF Conference on Computer Vision and Pattern Recognition*, pp. 3749–3761, 2022.
- Ju He, Enyu Zhou, Liusheng Sun, Fei Lei, Chenyang Liu, and Wenxiu Sun. Semi-synthesis: A fast way to produce effective datasets for stereo matching. In *Proceedings of the IEEE/CVF Conference on Computer Vision and Pattern Recognition*, pp. 2884–2893, 2021.

- Wenlong Huang, Pieter Abbeel, Deepak Pathak, and Igor Mordatch. Language models as zero-shot planners: Extracting actionable knowledge for embodied agents. In *International Conference on Machine Learning*, pp. 9118–9147, 2022.
- Wenlong Huang, Chen Wang, Ruohan Zhang, Yunzhu Li, Jiajun Wu, and Li Fei-Fei. VoxPoser: Composable 3D value maps for robotic manipulation with language models. *arXiv preprint arXiv:2307.05973*, 2023.
- Shima Imani, Liang Du, and Harsh Shrivastava. Mathprompter: Mathematical reasoning using large language models. *arXiv preprint arXiv:2303.05398*, 2023.
- Ajay Jain, Ben Mildenhall, Jonathan T Barron, Pieter Abbeel, and Ben Poole. Zero-shot text-guided object generation with dream fields. In *Proceedings of the IEEE/CVF Conference on Computer Vision and Pattern Recognition*, pp. 867–876, 2022.
- Katharina Jeblick, Balthasar Schachtner, Jakob Dexl, Andreas Mittermeier, Anna Theresa Stüber, Johanna Topalis, Tobias Weber, Philipp Wesp, Bastian Sabel, Jens Ricke, and Michael Ingrisch. ChatGPT makes medicine easy to swallow: An exploratory case study on simplified radiology reports. *arXiv preprint arXiv:2212.14882*, 2022.
- Chenfanfu Jiang, Siyuan Qi, Yixin Zhu, Siyuan Huang, Jenny Lin, Lap-Fai Yu, Demetri Terzopoulos, and Song-Chun Zhu. Configurable 3D scene synthesis and 2D image rendering with per-pixel ground truth using stochastic grammars. *International Journal of Computer Vision*, 126:920–941, 2018.
- Chen-Hsuan Lin, Jun Gao, Luming Tang, Towaki Takikawa, Xiaohui Zeng, Xun Huang, Karsten Kreis, Sanja Fidler, Ming-Yu Liu, and Tsung-Yi Lin. Magic3D: High-resolution text-to-3D content creation. In *Proceedings of the IEEE/CVF Conference on Computer Vision and Pattern Recognition*, pp. 300–309, 2023.
- Minghua Liu, Chao Xu, Haian Jin, Linghao Chen, Zexiang Xu, Hao Su, et al. One-2-3-45: Any single image to 3D mesh in 45 seconds without per-shape optimization. *arXiv preprint arXiv:2306.16928*, 2023.
- Luke Melas-Kyriazi, Christian Rupprecht, Iro Laina, and Andrea Vedaldi. Realfusion: 360 reconstruction of any object from a single image. In *Proceedings of the IEEE/CVF conference on computer vision and pattern recognition*, 2023.
- Sachit Menon and Carl Vondrick. Visual classification via description from large language models. *arXiv preprint arXiv:2210.07183*, 2022.
- Gal Metzer, Elad Richardson, Or Patashnik, Raja Giryes, and Daniel Cohen-Or. Latent-NeRF for shape-guided generation of 3D shapes and textures. In *Proceedings of the IEEE/CVF Conference on Computer Vision and Pattern Recognition*, pp. 12663–12673, 2023.
- Ben Mildenhall, Pratul P Srinivasan, Matthew Tancik, Jonathan T Barron, Ravi Ramamoorthi, and Ren Ng. NeRF: Representing scenes as neural radiance fields for view synthesis. *Communications of the ACM*, 65(1):99–106, 2021.
- Nasir Mohammad Khalid, Tianhao Xie, Eugene Belilovsky, and Tiberiu Popa. CLIP-Mesh: Generating textured meshes from text using pretrained image-text models. In *SIGGRAPH Asia 2022 conference papers*, pp. 1–8, 2022.
- OpenAI. GPT-4 technical report, 2023.
- Ben Poole, Ajay Jain, Jonathan T Barron, and Ben Mildenhall. DreamFusion: Text-to-3D using 2D diffusion. *arXiv preprint arXiv:2209.14988*, 2022.
- Sarah Pratt, Ian Covert, Rosanne Liu, and Ali Farhadi. What does a platypus look like? generating customized prompts for zero-shot image classification. *arXiv preprint arXiv:2209.03320*, 2022.
- Alec Radford, Jong Wook Kim, Chris Hallacy, Aditya Ramesh, Gabriel Goh, Sandhini Agarwal, Girish Sastry, Amanda Askell, Pamela Mishkin, Jack Clark, et al. Learning transferable visual models from natural language supervision. In *International conference on machine learning*, pp. 8748–8763. PMLR, 2021.

- Colin Raffel, Noam Shazeer, Adam Roberts, Katherine Lee, Sharan Narang, Michael Matena, Yanqi Zhou, Wei Li, and Peter J. Liu. Exploring the limits of transfer learning with a unified text-to-text transformer. *Journal of Machine Learning Research*, 21(140):1–67, 2020.
- Alexander Raistrick, Lahav Lipson, Zeyu Ma, Lingjie Mei, Mingzhe Wang, Yiming Zuo, Karhan Kayan, Hongyu Wen, Beining Han, Yihan Wang, Alejandro Newell, Hei Law, Ankit Goyal, Kaiyu Yang, and Jia Deng. Infinite photorealistic worlds using procedural generation. In *Proceedings of the IEEE/CVF Conference on Computer Vision and Pattern Recognition*, pp. 12630–12641, 2023.
- Amit Raj, Srinivas Kaza, Ben Poole, Michael Niemeyer, Ben Mildenhall, Nataniel Ruiz, Shiran Zada, Kfir Aberman, Michael Rubenstein, Jonathan Barron, Yuanzhen Li, and Varun Jampani. DreamBooth3D: Subject-driven text-to-3D generation. In *Proceedings of the International Conference on Computer Vision*, 2023.
- Robin Rombach, Andreas Blattmann, Dominik Lorenz, Patrick Esser, and Björn Ommer. High-resolution image synthesis with latent diffusion models. In *Proceedings of the IEEE/CVF conference on computer vision and pattern recognition*, pp. 10684–10695, 2022.
- Aditya Sanghi, Hang Chu, Joseph G Lambourne, Ye Wang, Chin-Yi Cheng, Marco Fumero, and Kamal Rahimi Malekshan. CLIP-Forge: Towards zero-shot text-to-shape generation. In *Proceedings of the IEEE/CVF Conference on Computer Vision and Pattern Recognition*, pp. 18603–18613, 2022.
- Ross Taylor, Marcin Kardas, Guillem Cucurull, Thomas Scialom, Anthony Hartshorn, Elvis Saravia, Andrew Poultion, Viktor Kerkez, and Robert Stojnic. Galactica: A large language model for science. *arXiv preprint arXiv:2211.09085*, 2022.
- Romal Thoppilan, Daniel De Freitas, Jamie Hall, Noam Shazeer, Apoorv Kulshreshtha, Heng-Tze Cheng, Alicia Jin, Taylor Bos, Leslie Baker, Yu Du, YaGuang Li, Hongrae Lee, Huaixiu Steven Zheng, Amin Ghafouri, Marcelo Menegali, Yanping Huang, Maxim Krikun, Dmitry Lepikhin, James Qin, Dehao Chen, Yuanzhong Xu, Zhifeng Chen, Adam Roberts, Maarten Bosma, Vincent Zhao, Yanqi Zhou, Chung-Ching Chang, Igor Krivokon, Will Rusch, Marc Pickett, Pranesh Srinivasan, Laichee Man, Kathleen Meier-Hellstern, Meredith Ringel Morris, Tulsee Doshi, Renelito Delos Santos, Toju Duke, Johnny Soraker, Ben Zevenbergen, Vinodkumar Prabhakaran, Mark Diaz, Ben Hutchinson, Kristen Olson, Alejandra Molina, Erin Hoffman-John, Josh Lee, Lora Aroyo, Ravi Rajakumar, Alena Butryna, Matthew Lamm, Viktoriya Kuzmina, Joe Fenlon, Aaron Cohen, Rachel Bernstein, Ray Kurzweil, Blaise Aguera-Arcas, Claire Cui, Marian Croak, Ed Chi, and Quoc Le. Lamda: Language models for dialog applications. *arXiv preprint arXiv:2201.08239*, 2022.
- Zhengyi Wang, Cheng Lu, Yikai Wang, Fan Bao, Chongxuan Li, Hang Su, and Jun Zhu. Prolific-Dreamer: High-fidelity and diverse text-to-3d generation with variational score distillation. *arXiv preprint arXiv:2305.16213*, 2023.
- Jason Wei, Xuezhi Wang, Dale Schuurmans, Maarten Bosma, Brian Ichter, Fei Xia, Ed Chi, Quoc Le, and Denny Zhou. Chain-of-thought prompting elicits reasoning in large language models. *Advances in Neural Information Processing Systems*, 35:24824–24837, 2022.
- Jiale Xu, Xintao Wang, Weihao Cheng, Yan-Pei Cao, Ying Shan, Xiaohu Qie, and Shenghua Gao. Dream3D: Zero-shot text-to-3D synthesis using 3D shape prior and text-to-image diffusion models. In *Proceedings of the IEEE/CVF Conference on Computer Vision and Pattern Recognition*, pp. 20908–20918, 2023.
- Kailai Yang, Shaowiong Ji, Tianlin Zhang, Qianqian Xie, and Sophia Ananiadou. On the evaluations of ChatGPT and emotion-enhanced prompting for mental health analysis. *arXiv preprint arXiv:2304.03347*, 2023.
- Andy Zeng, Maria Attarian, Brian Ichter, Krzysztof Choromanski, Adrian Wong, Stefan Welker, Federico Tombari, Aveek Purohit, Michael Ryoo, Vikas Sindhwani, Johnny Lee, Vincent Vanhoucke, and Pete Florence. Socratic models: Composing zero-shot multimodal reasoning with language. *arXiv preprint arXiv:2204.00598*, 2022.

Ceyao Zhang, Kaijie Yang, Siyi Hu, Zihao Wang, Guanghe Li, Yihang Sun, Cheng Zhang, Zhaowei Zhang, Anji Liu, Song-Chun Zhu, Xiaojun Chang, Junge Zhang, Feng Yin, Yitao Liang, and Yaodong Yang. Proagent: Building proactive cooperative ai with large language models. *arXiv preprint arXiv:2308.11339*, 2023a.

Lvmin Zhang, Anyi Rao, and Maneesh Agrawala. Adding conditional control to text-to-image diffusion models. In *IEEE International Conference on Computer Vision (ICCV)*, 2023b.

6 APPENDIX

6.1 ADDITIONAL RESULT

We kindly request the reader to consider visiting <https://chuny1.github.io/3DGPT/3dgpt.html> to view our high-quality 3D results.

6.2 PROMPT EXAMPLE

We offer an illustrative example of the prompt used for Adding Trees, presenting the Document, Code, Information, and a Usage Example.

Document:
Explanation: The function takes a built natural scene as input and adds base trees to it.
Inputs:
scene: The built natural scene. density(float): The density of the trees. distance_min(float): Minimum distance between trees. leaf_type(string): The type of leaf on the tree. Select one from the list ['leaf', 'leaf_broadleaf', 'leaf_ginko', 'leaf_maple', 'flower', 'None']. 'Leaf' allows further custom settings like changing the leaf shape and color. 'Leaf_broadleaf', 'leaf_ginko', and 'leaf_maple' build the leaves with predefined shapes: broad, ginko, and maple respectively. 'Flower' will create flowers on the tree instead of leaves. 'None' will not generate leaves on the tree. fruit_type(string): The type of fruit on the tree. Select one from the list ['apple', 'blackberry', 'coconut_green', 'durian', 'starfruit', 'strawberry', 'custom_fruit', 'None']. Each of the fruit types will create the corresponding fruit on the tree. 'Custom_fruit' can create customizable fruit on the tree with further adjustments. If the desired fruit is not on the list, 'custom_fruit' should be chosen. 'None' will not generate any fruit on the tree.
Code:
<pre>'''python import TreeFactory def add_trees(scene, density, distance_min, leaf_type, fruit_type, leaf_density): trees = TreeFactory.create(density, leaf_type, fruit_type, leaf_density) # create trees scene.place(trees, distance_min) # place trees in the scene return '''</pre>
Information:
"Possible trees in the scene, tree types, leaf density, possible seasons, tree size, appearance of the tree branch, branch type, and leaf color."
Example:
Question: Given the text description of the scene, analyze the function parameters and call the function to add more trees that fit the text description. Solution: From the text description, three different types of trees are identified in the scene: birch, dogwood, and Japanese maple. From "a cluster of," we infer the tree density is relatively high; let's set it to 0.2. Birch tree leaves are typically oval or triangular, so let's set the leaf type to 'leaf' to allow further customization. There are no fruits mentioned for the birch tree in the description. Given the scene likely depicts autumn, the leaf_density should not be too high; let's set it to 0.02. For the dogwood tree, as the leaves are described as oval or elliptical with smooth edges, the leaf type is set to 'leaf'. It is mentioned that "clusters of small, vibrant berries cling to its branches," so we can choose the fruit_type as 'blackberry'. The leaf_density is set to 0.02. For the Japanese maple tree, the leaf type is set to 'leaf_maple'. No fruits are mentioned for the maple tree. As the scene likely takes place in autumn, the leaf density for the maple tree should be high; let's set it to 0.1. The function can be called three times to create three different trees: <pre>'''python add_trees(scene, density=0.2, distance_min=1, leaf_type='leaf', fruit_type='None', leaf_density=0.02) # create birch trees add_trees(scene, density=0.1, distance_min=1, leaf_type='leaf', fruit_type='blackberry', leaf_density=0.02) # create dogwood trees add_trees(scene, density=0.1, distance_min=1, leaf_type='leaf_maple', fruit_type='None', leaf_density=0.1) # create Japanese maple trees '''</pre>

Figure 7: Prompt Example of Adding Trees.

Document: Input: sun_intensity: Multiplier for sun disc lighting. (Choose from 'low', 'median', 'high') sun_elevation: Rotation of the sun from the horizon (in degrees). (0: sunset, sun rising, 90: daytime, -10: night) sun_rotation: Rotation of the sun around the zenith (in degrees). air_density: Density of air molecules. (0: no air, 1: clear day atmosphere, 2: highly polluted day) dust_density: Density of dust and water droplets. (0: no dust, 1: clear day atmosphere, 5: city-like atmosphere, 10: hazy day) ozone: Density of ozone molecules; useful to make the sky appear bluer. (0: no ozone, 1: clear day atmosphere, 2: city-like atmosphere). A higher value yields a bluer sky. cloud_density: Density of the clouds, ranging from 0 to 0.04. (0.01: very thick cloud, 0.04: very heavy cloud) Output: texture_color_output: The output texture color of the sky.
Code: <pre>'''python import nishita_sky_modelling def sky_texture_node(sun_intensity, sun_elevation, sun_rotation, air_density, dust_density, ozone, cloud_density): texture = nishita_sky_modelling.model_sky(sun_intensity, sun_elevation, sun_rotation, air_density, dust_density, ozone, cloud_density) return texture '''</pre>
Information: The time of day depicted in the scene (morning/noon/evening), the possible season, the condition of the air, the blueness of the sky, and the cloud density.
Example: Question: Given the text description of the scene: "The river, reflecting the clear blue of the sky, glistened like a silver ribbon as it wound its way through the lush valley, its tranquil waters whispering secrets to the ancient trees." analyze the function parameters and call the function to generate the sky. Solution: From the description of a "clear blue sky," we infer that sun_intensity cannot be low, let's set it as "median". As the sky is clear and blue, the sun_elevation must not be very low, indicating it's not morning or evening; we can set it to 50 degrees. Sun rotation does not impact the appearance of the sky significantly; thus, we will set it to 0 degrees. To align with the description of "clear blue," we should choose lower values for air_density and dust_density. Hence, we will set air_density to 1 and dust_density to 0. To enhance the blueness of the sky, we can increase the ozone value to 2. As the description suggests a clear, blue sky, the cloud density must be low. Therefore, we will set it to 0.0005. The sky can be modeled by invoking the function as follows: <pre>'''python sky_texture_node(sun_intensity='median', sun_elevation=50, sun_rotation=0, air_density=1, dust_density=0, ozone=2, cloud_density=0.0005) '''</pre>

Figure 8: Prompt Example of Sky Modeling Function.

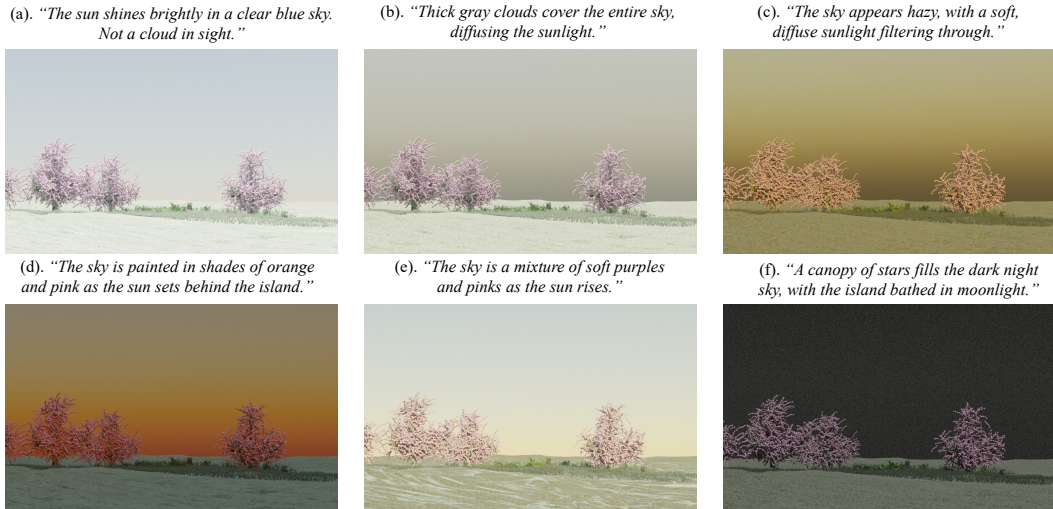
6.3 ABLATION STUDY DETAILS

We conduct separate ablation studies for the Conceptualization Agent and Task Dispatch Agent, evaluating their performance based on CLIP scores, failure rates, and parameter diversity.

We use the implementation of Radford et al. (2021) to calculate CLIP score. It measures cosine similarity in the CLIP hidden space, indicating the alignment between generated images and text descriptions. For 3D scene CLIP scores, we placed a camera at the scene's center, capturing 50 images by rotating the camera 360 degrees. In the Conceptualization Agent evaluation, we used only the initial instruction. For the Task Dispatch Agent, both the initial instruction and one subsequent instruction were used.

The failure rate reflects the Modeling Agent's response. Failures can occur when the method cannot extract the correct pattern via the parser, generates data with an incorrect datatype, or omits/adds parameters to the function call. We evaluated five functions for each scene, recording the failure rate. We also assessed 500 parameters per scene, employing the Shannon Diversity Index to measure parameter diversity, and categorizing float parameters into 100 bins.

6.4 AGENT RESPONSES AND VISUAL RESULT



(a). Solution: From the description of "clear blue sky" and "not a cloud in sight", we can infer that the sun_intensity should be high, the sun_elevation should be around 90 (daytime), the sun_rotation can be set to 0. The air_density and dust_density should be low, so we can set them to 1 and 0 respectively. Since there are no clouds, the cloud_density should be 0. To make the sky appear bluer, we can increase the ozone value, so let's set it to 2. We can model the sky by calling the following function:

```
'''python
sky_texture_node(sun_intensity='high', sun_elevation=90, sun_rotation=0, air_density=1, dust_density=0, ozone=2, cloud_density=0)
'''
```

(b). Solution: From the description of "Thick gray clouds cover the entire sky", the sun_intensity should be low to account for the diffused sunlight. Let's set it as "low". The sun_elevation should be high to indicate that it is daytime. Let's set it to 90. The sun_rotation does not affect the sky appearance, so we can set it to 0. The air_density and dust_density should be high to represent the presence of thick clouds. Let's set air_density to 2 and dust_density to 5. Since the sky is covered with thick gray clouds, the ozone value can be low. Let's set it to 0. As mentioned, the entire sky is covered with thick gray clouds, so the cloud_density should be high. Let's set it to 0.04. We can model the sky by calling the following function:

```
'''python
sky_texture_node(sun_intensity='low', sun_elevation=90, sun_rotation=0, air_density=2, dust_density=5, ozone=0, cloud_density=0.04)
'''
```

(c). Solution: From the description of "hazy sky" and "soft, diffuse sunlight", we can infer that the sun_intensity should be low. Let's set it as "low". The sun_elevation should be low as well, indicating a time close to sunrise or sunset. Let's set it to -10. The sun_rotation does not affect the sky appearance, so we can set it to 0. To fit the description of a hazy sky, the air_density and dust_density should be higher. Let's set air_density to 2 and dust_density to 5. The ozone value can be set to 1 to maintain a natural sky color. Since the sky is hazy, the cloud_density should be higher as well. Let's set it to 0.02 to represent a moderately cloudy sky. We can model the sky by calling the following function:

```
'''python
sky_texture_node(sun_intensity='low', sun_elevation=-10, sun_rotation=0, air_density=2, dust_density=5, ozone=1, cloud_density=0.02)
'''
```

(d). Solution: From the description of "shades of orange and pink", the sun_intensity can be set as "low" to create a softer and warmer lighting. As the sun is setting, the sun_elevation can be set to 0. The sun_rotation does not affect the sky appearance, so it can be set to 0. To fit the description of "shades of orange and pink", the air_density and dust_density should be low, so we can set air_density to 1 and dust_density to 0. To create a warmer and more vibrant sky, we can set the ozone value to 1. As the sun is setting, there might be some clouds in the sky, so we can set the cloud_density to 0.01. We can model the sky by calling the following function:

```
'''python
sky_texture_node(sun_intensity='low', sun_elevation=0, sun_rotation=0, air_density=1, dust_density=0, ozone=1, cloud_density=0.01)
'''
```

(e). Solution: From the description of "soft purples and pinks", the sun_intensity can be set to "low" to create a softer lighting effect. Since the sun is rising, the sun_elevation can be set to a low value, such as 10. The sun_rotation does not affect the sky appearance, so it can be set to 0. To create a purple and pink sky, the air_density and dust_density can be set to low values, such as 1 and 0. The ozone value can be set to 0 to avoid making the sky bluer. Since the sky is described as a mixture of colors, the cloud_density can be set to a low value, such as 0.001. We can model the sky by calling the following function:

```
'''python
sky_texture_node(sun_intensity='low', sun_elevation=10, sun_rotation=0, air_density=1, dust_density=0, ozone=0, cloud_density=0.001)
'''
```

(f). Solution: From the description of "dark night sky" and "canopy of stars", we can assume that the sun is not visible in the sky. Therefore, the sun_intensity can be set to 'low'. Since it is a night scene, the sun_elevation can be set to -10. The sun_rotation does not affect the sky appearance, so it can be set to 0. As it is a dark night sky, the air_density and dust_density can be set to 0. The ozone value can also be set to 0 as there is no mention of blueness in the description. Since there are no clouds mentioned, the cloud_density can be set to 0. We can model the sky by calling the following function:

```
'''python
sky_texture_node(sun_intensity='low', sun_elevation=-10, sun_rotation=0, air_density=0, dust_density=0, ozone=0, cloud_density=0)
'''
```

Figure 9: **Single Function Control Result.** Visual result (top) and modeling agent response example (bottom). Our method demonstrates a high degree of accuracy in inferring algorithm parameters, even when they do not possess a direct connection to visual appearance.